Chinese Journal of Catalysis 38 (2017) 1373–1381

available at www.sciencedirect.com

ScienceDirect

journal homepage: www.elsevier.com/locate/chnjc

Article

Tuning the growth of Cu-MOFs for efficient catalytic hydrolysis of carbonyl sulfide

Lijuan Shen, Gaojie Wang, Xiaoxiao Zheng, Yanning Cao, Yufeng Guo, Ke Lin, Lilong Jiang *

National Engineering Research Center of Chemical Fertilizer Catalyst, Fuzhou University, Fuzhou 350002, Fujian, China

ARTICLE INFO

Article history:
Received 11 April 2017
Accepted 17 June 2017
Published 5 August 2017

Keywords:
Metal-organic framework
Carbonyl sulfide
Electrochemical synthesis
Catalytic hydrolysis
HKUST-1

ABSTRACT

Development of the high activity, promoter-free catalysts for carbonyl sulfide (COS) hydrolysis is important for the efficient utilization of various feedstocks. In this study, the Cu-based metal-organic framework HKUST-1 is synthesized by a simple and mild anodic-dissolution electrochemical method. The physical and chemical properties of the samples are characterized by several techniques, including scanning electron microscopy, X-ray diffraction, Brunauer-Emmett-Teller analysis and X-ray photoelectron spectroscopy. The results reveal that the synthesis voltage plays a crucial role in controlling the morphology of the resulting HKUST-1. The obtained samples function as novel catalysts for the hydrolysis of COS. A high efficiency, approaching 100%, can be achieved for the conversion of COS at 150 °C over the optimal HKUST-1 synthesized at 25 V. This is significantly higher than that of the sample prepared by the traditional hydrothermal method. Additionally, the effects of the water temperature and the flow velocity on the hydrolysis of COS are also investigated in detail. Finally, a possible reaction pathway of COS hydrolysis over HKUST-1 is also proposed. This work represents the first example of MOFs applied to the catalytic hydrolysis of COS. The results presented in this study can be anticipated to give a feasible impetus to design novel catalysts for removing the sulfur-containing compounds.

1. Introduction

Sulfur compounds are frequently present in petroleum gas, water gas, and natural gas, where they not only corrode reaction equipment and deactivate catalysts but also cause damage to the environment as major sources of acid rain [1–4]. In particular, carbonyl sulfide (COS) is probably the most long-lived sulfur gas because of its chemical stability [5,6]. In view of both increasingly stringent environmental regulations and the technical requirements of further catalytic processes, the removal of COS is of high urgency. Several methods, including adsorption, reduction, oxidation and hydrolysis, have been developed to remove COS [7]. Among them, hydrolysis ($COS + H_2O \rightarrow H_2S + CO_2$) is recognized as the most promising process by virtue of its mild reaction conditions and high conversion efficiency [8,9]. Previous studies have been devoted to the development of catalysts for COS hydrolysis, mostly focusing on metal oxides like titania and alumina [10–12]. In order to improve the activities of these catalysts, alkali earth metals, transition metal oxides (Co, Cu, Ni, Fe, Zn) and rare earth metal oxides are often used as promoters [13–15]. Additionally, carbon materials have been reported as promising catalysts for COS hydrolysis. For example, Ning et al. [16] reported that in the hydrolysis of COS over activated carbon, the catalytic activity was enhanced by

---

* Corresponding author. Tel: +86-591-83731234; E-mail: jll@fzu.edu.cn

This work was supported by the National Natural Science Foundation of China (21603034, 21576051) and the National High Technology Research and Development Program of China (863 Program, 2015AA03A402).

DOI: 10.1016/S1872-2067(17)62874-2 | http://www.sciencedirect.com/science/journal/18722067 | Chin. J. Catal., Vol. 38, No. 8, August 2017

adding Fe, Cu, Ni or Ce promoters. Although these systems have beneficial features, the search for new catalysts with high activity and without the need for promoters remains an active research challenge.

Among various materials, metal-organic frameworks (MOFs), which are assembled by combining metal ions/clusters with organic ligands, have attracted particular attention [17–19]. The unique features of MOFs, such as high pore volumes, high specific surface areas and structural flexibility, make them attractive candidates for applications including adsorption [20–22], separation [23], chemical sensing and drug release [24,25]. In particular, MOFs are promising in the field of catalysis [26–31]. Their accessible open-metal centers, as well as functional groups incorporated into the linkers, can function as active sites, endowing them with catalytic properties. Distinct from conventional catalysts, MOFs can be synthesized from materials with well-defined crystalline structures. This is beneficial for the characterization of these catalysts and may provide new opportunities for a deep study of their structure-property relationships. Moreover, the properties of MOFs can be facilely controlled through the modification of the metal center or organic linker because of their adaptable chemistry, enabling them to be easily tailored to meet specific needs [32–34]. Despite the rapidly growing interest in MOFs, however, to the best of our knowledge, no previous work regarding their application for the catalytic hydrolysis of COS has been reported.

Herein, we report the synthesis of the Cu-based MOF HKUST-1 by the anodic-dissolution method and its application for COS hydrolysis. HKUST-1 is constructed by Cu^{2+} ions coordinated to the 1,3,5-benzenetricarboxylate ligand, forming a 3D, porous, square-shaped (0.9 nm × 0.9 nm) structure [35,36]. HKUST-1 is chosen as the target of research for several reasons. First, the proper pore sizes are ideal for the adsorption and diffusion of COS molecules. Second, the coordinatively unsaturated copper centers and the high stability of HKUST-1 are beneficial for catalysis. Finally, the synthesis of HKUST-1 requires only inexpensive copper sources and trimesic acid, and it is already commercially available, suggesting that HKUST-1 could fulfill the requirements for industrial use [37]. Compared with the traditional methods, which require high energy consumption and long reaction time, the electrochemical synthesis consumes less energy while effectively shortening the reaction time (from a matter of days to a few hours). More significantly, it offers the ability to influence the reaction directly in real-time, allowing more control of the reaction throughout the process [38–40]. Herein, the synthesis of HKUST-1 is controlled by varying the synthesis voltage, and the product is structurally characterized by XRD, SEM, BET and XPS. It is found that the as-synthesized samples exhibit excellent activity for the catalytic hydrolysis of COS.

2. Experimental

2.1. Preparation

2.1.1. Materials

Copper rod (19 mm diam, 56 g, purity = 99.9998%) as electrode material and tetrabutylammonium perchlorate (TBAP; purity > 99%) as supporting electrolyte were purchased from Sigma Aldrich Co., Ltd. (Shanghai, China). 1,3,5-Benzenetricarboxylic acid (H_3BTC; purity >99%) was supplied by Beijing Lark Technology Co., Ltd., China. Ethanol (C_2H_5OH) was purchased from Sinopharm Chemical Reagent Co., Ltd. (Shanghai, China). Deionized (DI) water was obtained from local sources. All of the above chemicals were used as received and without further purification.

2.1.2. Synthesis of HKUST-1 by electrochemical method

Two copper electrodes were used as anode and cathode, respectively, for the synthesis of HKUST-1. The organic linker (1.75 g H_3BTC) and supporting electrolyte (2.85 g TBAP) were dissolved in 240 mL ethanol/water (3:1) solution. Electrolysis was carried out in a self-contained electrochemical cell under constant voltages (15, 20, 25 and 30 V) that were held for 3 h, following which products blue in color were obtained. After that, the samples were washed three times with water and ethanol separately, and then dried in an oven at 100 °C for 24 h. Finally, a series of HKUST-1 samples was obtained. According to the voltage used during the synthesis, the obtained samples were named as HKUST-1-E15, HKUST-1-E20, HKUST-1-E25 and HKUST-1-E30, respectively.

2.1.3. Synthesis of HKUST-1 by solvothermal method

For comparison purposes, HKUST-1 was also prepared by the solvothermal method [41]. $Cu(NO_3)_2\cdot 3H_2O$ (2.077 g) was dissolved in 15 mL deionized water. Separately, H_3BTC (1.00 g) was dissolved in 30 mL *N*,*N*-dimethylformamide/ethanol solution (1:1). Then, the above two solutions were mixed and stirred for 10 min. After that, the mixture was transferred to a 70 mL Teflon-lined stainless-steel autoclave, then heated to 100 °C and held for 12 h. After cooling to room temperature, it was filtered and washed three times with water and ethanol separately, and then dried in an oven at 100 °C for 24 h. The obtained sample was named as HKUST-1-Hy.

2.2. Characterizations

The as-synthesized HKUST-1 was characterized by X-ray diffraction (XRD, X'Pert PRO) using Co K_α radiation (λ = 0.1790 nm), with a voltage of 40 kV and current of 40 mA. The morphologies and microstructures of HKUST-1 were studied by scanning electron microscope (SEM, S-4800, Hitachi, Japan) analysis. The Brunauer-Emmett-Teller (BET) surface areas and average pore diameters of the HKUST-1 were measured by N_2 adsorption-desorption using an ASAP 2020 instrument (Micromeritics, USA). FT-IR spectra were recorded over a Nicolet 6700 spectrometer (Thermo Fisher Scientific) with an MCT detector. Nitrogen was introduced into the IR cell as the background. The spectra were obtained in the 4000–800 cm^{-1} range at a resolution of 2.0 cm^{-1} with 32 scans. X-ray photoelectron spectroscopy (XPS) measurements were performed over a PHI Quantum 2000 XPS system.

2.3. Evaluation of catalytic activity

The hydrolysis of COS over HKUST-1 was performed in a fixed-bed reactor at atmospheric pressure. 0.4 g catalyst was used. At steady state, a mixture gas of N_2 containing COS (100 mg/m^3) was introduced into the reactorat a total flow rate of 30 mL/min. H_2O was injected from a thermostatic water bath through a controlled saturator. By adjusting the temperature of the water bath, the relative humidity of the reaction gas was controlled. The concentration of COS in the reactor effluent was monitored on-line by a gas chromatograph (Shimadzu GC 2014) equipped with a flame photometric detector. The conversion of COS was determined by analyzing the initial and the current temperature-peak areas of COS in the GC. In this study, the COS conversion was calculated as follows:

$$\text{COS conversion (\%)} = (C_0 - C_T) / C_0 \times 100$$

where C_0 and C_T are the peak area of COS at temperatures of 30 °C and T °C, respectively.

3. Results and discussion

3.1. SEM

The morphologies and microstructures of HKUST-1 were investigated by SEM. As shown in Fig. 1, the synthesis voltage of the reaction system greatly affected the morphologies of HKUST-1. HKUST-1-E15 shows a rod-like morphology with rod lengths of about 15 μm. As the voltage increases, the structure becomes progressively shorter, and the rod-like morphology gradually transforms to an octahedral shape for the sample of HKUST-1-E25. With the further increase of the voltage to 30 V, the crystal size of HKUST-1-E30 decreases and the particles aggregate into an irregular structure. Note that the particle sizes of the HKUST-1 samples synthesized electrochemically are non uniform. This may have arisen from the concentration gradient of Cu^{2+} in the reaction system, whereby the electrolyte provides a higher concentration of Cu^{2+} around the copper anode.

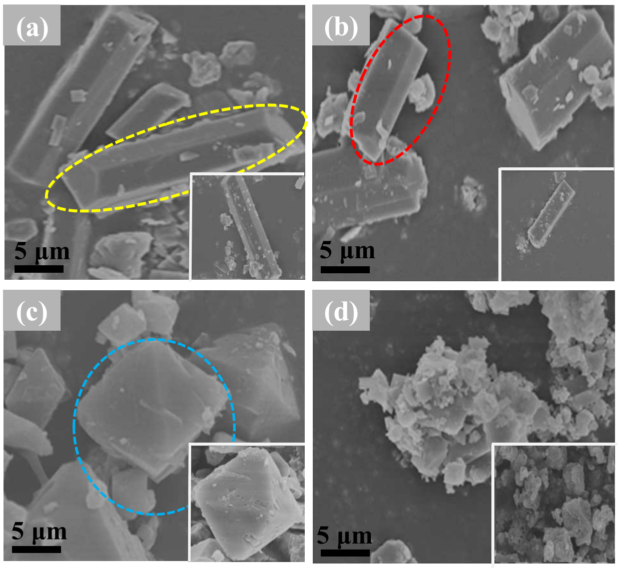

Fig. 1. SEM images of HKUST-1-E15 (a), HKUST-1-E20 (b), HKUST-1-E25 (c) and HKUST-1-E30 (d).

3.2. XRD

Fig. 2 shows the powder XRD patterns of HKUST-1 synthesized at different voltages. The diffraction peaks of all the as-synthesized HKUST-1 samples match the simulated pattern, confirming the successful synthesis of HKUST-1 by electrochemical anodic dissolution. With the increase of the voltage from 15 to 25 V, the intensity of the diffraction peaks of the samples gradually increases. The sharp diffraction peaks of HKUST-1-E25 indicate its high crystallinity. With the further increase of the voltage to 30 V, the diffraction peaks of HKUST-1-E30 decrease in intensity. Moreover, additional peaks are observed, which possibly arise from the formation of a small amount of Cu_2O [42]. Comparing the four samples of HKUST-1, the dominant facets are found to be slightly different in each case. As is known, the growth of crystals is coordinated by the cooperative growth of some planes at slower speeds and others at faster speeds, and the exposed facets of the crystal are generally the slower-growing planes [43]. The above results indicate the significant influence of the voltage on the growth of these MOF crystals. This is in good agreement with the SEM results.

3.3. BET

Fig. 3 shows the N_2 adsorption-desorption isotherms and pore size distributions of HKUST-1 synthesized at different voltages. The type I adsorption isotherm of HKUST-1-E15 suggests the existence of micropores in this sample. For HKUST-1-E20 and HKUST-1-E25, it can be seen that besides the adsorption capacity in the area of low pressure, both samples also display a hysteresis loop in the areas of medium and high pressure. The curves show the properties of I/IV mixed-type isotherms, indicating the presence of micropores and meso-

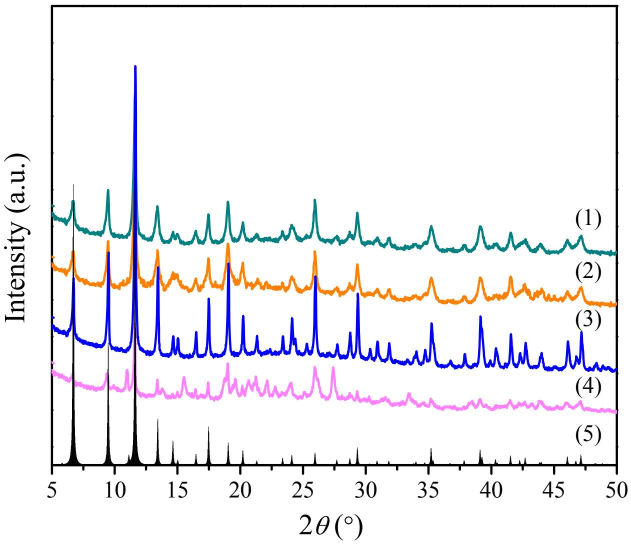

Fig. 2. XRD patterns of HKUST-1-E15 (1), HKUST-1-E20 (2), HKUST-1-E25 (3), HKUST-1-E30 (4), and simulated HKUST-1 (5).

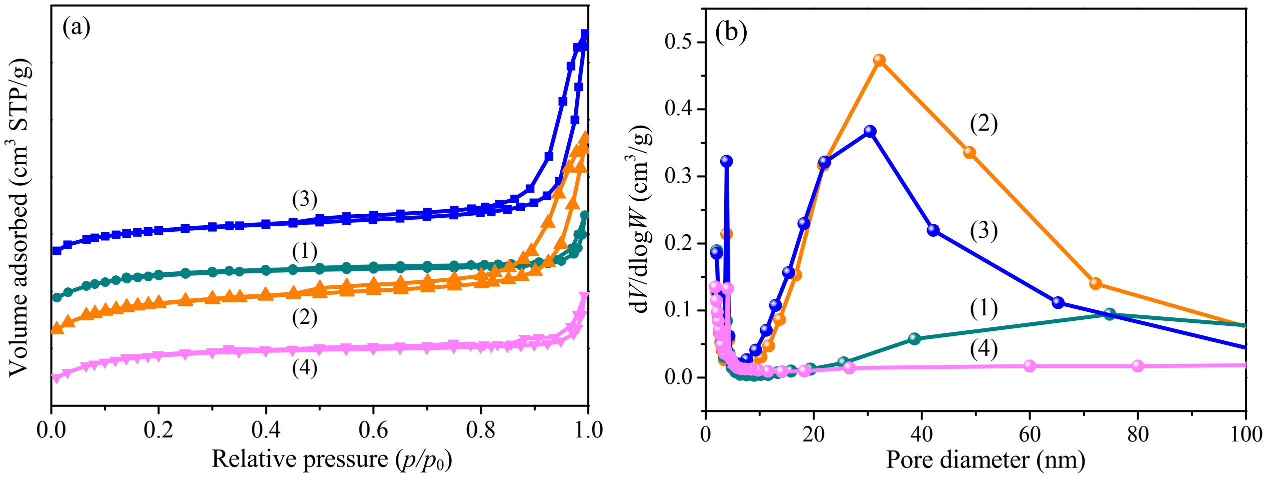

Fig. 3. N_2 adsorption-desorption isotherms (a) and pore size distributions (b) of HKUST-1-E15 (1), HKUST-1-E20 (2), HKUST-1-E25 (3), and HKUST-1-E30 (4).

pores. The mesopores of HKUST-1-E20 and HKUST-1-E25 are thought to be formed by the loose accumulation of HKUST-1 particles. For the sample of HKUST-1-E30, a type I microporous sorption isotherm is observed.

The corresponding textural parameters calculated from the N_2 adsorption-desorption isotherms are listed in Table 1. The BET surface area and pore volume of HKUST-1-E15 are 616 m^2/g and 0.17 cm^3/g, respectively, within the range of values reported in the literature [44]. As the voltage increases, the BET surface areas of the HKUST-1 increase. The BET surface areas are 738 and 786 m^2/g for HKUST-1-E20 and HKUST-1-E25, respectively. When further increasing the voltage to 30 V, the BET surface area of the obtained HKUST-1-E30 decreases to 405 m^2/g. These changes can be mainly attributed to the morphological and structural transformation of HKUST-1 with increasing voltage. It is expected that the HKUST-1 catalysts with greater specific surface area will be able to supply more surface active sites for the adsorption of COS, leading to enhanced catalytic performance.

3.4. COS hydrolysis performance

The catalytic performance of the as-synthesized HKUST-1 for the hydrolysis of COS was investigated at temperatures ranging from 30 to 150 °C. Before testing, control experiments were first carried out to verify the catalytic nature of the reactions. A blank experiment in the absence of catalyst led to no conversion of COS. Additionally, an experiment in the presence of catalyst was carried out at a constant temperature of 30 °C for 12 h. No obvious removal of COS was measured after reaching the adsorption–desorption equilibrium, which excludes the possibility that the mere adsorption of COS on HKUST-1 is responsible for its removal. In the presence of HKUST-1 catalyst, the COS is efficiently converted, as shown in Fig. 4. Increasing the reaction temperature results in an improvement of the COS conversion efficiency for each catalyst. At 30 °C, negligible COS conversion is obtained over all the HKUST-1 samples. When the temperature is increased to 150 °C, about 38% of the COS is hydrolyzed over HKUST-1-E15. Moreover, with increasing synthesis voltage, the catalytic activities of the obtained HKUST-1 are found to increase markedly. HKUST-1-E25 shows the highest activity, achieving a COS conversion efficiency of 98% at 150 °C. This conversion efficiency is also higher than that of the HKUST-1-Hy sample, which was prepared by the hydrothermal method. When the synthesis voltage was further increased to 30 V, the obtained HKUST-1-E30 sample shows much poorer activity, with a COS hydrolysis conversion efficiency of only 20%. This variation of catalytic activity with synthesis voltage may have been caused

Table 1
Textural properties of HKUST-1 synthesized at different voltages.

Sample	A_{BET} (m^2/g)	Pore volume (cm^3/g)	Average pore size (nm)
HKUST-1-E15	616	0.17	3.54
HKUST-1-E20	738	0.31	14.84
HKUST-1-E25	786	0.27	10.65
HKUST-1-E30	405	0.13	2.86

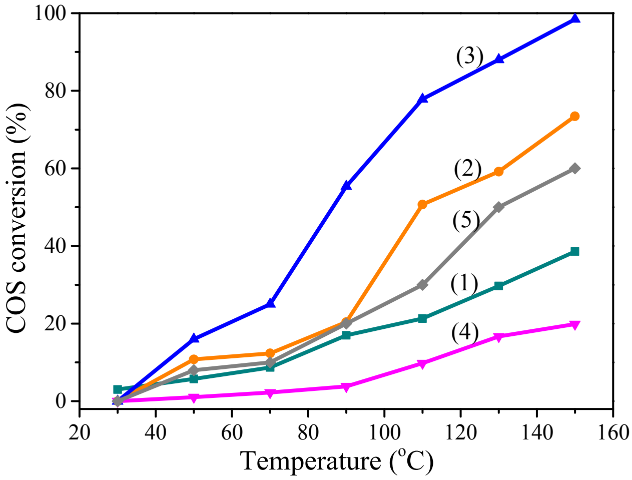

Fig. 4. COS hydrolysis over HKUST-1-E15 (1), HKUST-1-E20 (2), HKUST-1-E25 (3), HKUST-1-E30 (4), and HKUST-1-Hy (5). Reaction conditions: catalyst mass 0.4 g, feed gas 100 mg/cm^3 COS/N_2, WHSV 4500 h^{-1}, water temperature 40 °C.

by the corresponding structural changes of the HKUST-1. The products of the reaction included H_2S, as determined by chromatographic analysis. Moreover, the outlet gas was further collected and analyzed by IR spectroscopy. Absorption bands assigned to the (υ)3 mode of CO_2 were observed, confirming that the catalytic hydrolysis reaction had occurred [45]. To deduce the catalytic sites of HKUST-1, the catalytic activity of H_3BTC was also evaluated. In this case, the reaction did not proceed when an equivalent mass of H_3BTC was employed as a substitute for HKUST-1, suggesting that the open Cu sites (i.e., Cu^{2+}) of the HKUST-1 are the catalytic sites.

3.5. *Effect of the supporting electrolyte*

It is known that the synthesis parameters can affect the morphology and chemical properties of the resulting material. Therefore, besides the voltage, the influence of the supporting electrolyte on the growth of HKUST-1 was also investigated. A series of HKUST-1 was prepared at constant voltage (25 V) with different amounts of TBAP supporting electrolyte. The SEM analysis shows that these samples display a similar octahedral shape, with no significant differences in morphology among the three samples. The catalytic performance of this series of HKUST-1 was then evaluated, as shown in Fig. 5. The COS conversion efficiencies of the three samples are almost identical at all reaction temperatures: all three improve with increasing temperature and finally reach almost 100% at 150 °C, suggesting that the amount of supporting electrolyte has no obvious influence on the morphology and catalytic ability of HKUST-1.

3.6. *Effect of the water temperature*

As a reactant, the amount of water has a direct influence on the hydrolysis reaction. This can be adjusted by controlling the temperature of the water. Thus, it is also vital to determine the optimum water temperature. The effect of water temperature on the conversion of COS was investigated over the HKUST-1-E25 sample. As shown in Fig. 6, when the water temperature is 25 °C, the COS conversion efficiency is only about 70% at 150 °C because of the insufficient availability of water to participate in the reaction. When the water temperature is increased to 40 °C, nearly 100% COS is converted. However, further increasing the water temperature leads to decreased activity. When the water temperature is increased to 60 °C, the conversion efficiency of COS falls to 65%. This can be ascribed to the competitive adsorption between COS and H_2O on the surface of the catalyst. Excess water inhibits the chemisorption of COS, thus reducing the activity of the catalyst [46]. This result confirms that water temperature is a strongly influential factor on the hydrolysis of COS.

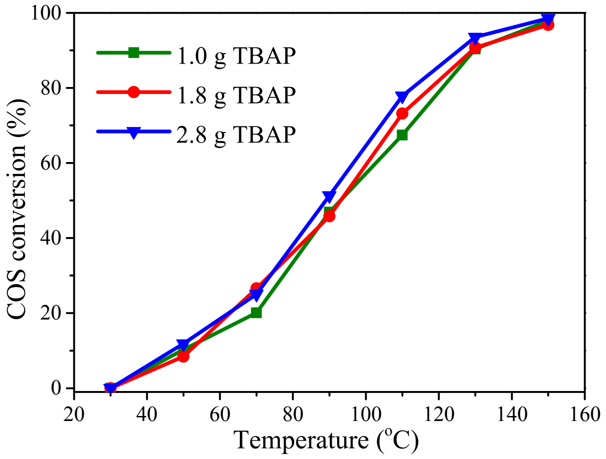

Fig. 5. COS hydrolysis over HKUST-1-E25 synthesized with different amounts of supporting electrolyte (TBAP). Reaction conditions: catalyst mass 0.4 g, feed gas 100 mg/cm³ COS/N_2, WHSV 4500 h^{-1}, water temperature 40 °C.

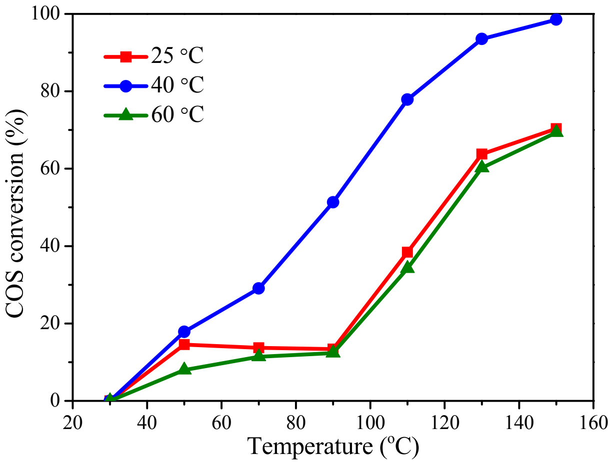

Fig. 6. Influence of water temperature on COS conversion over HKUST-1-E25. Reaction conditions: catalyst mass 0.4 g, feed gas 100 mg/cm³ COS /N_2, WHSV 4500 h^{-1}.

3.7. *Effect of the flow velocity*

Besides the water temperature, the effect of the feed gas flow velocity on the conversion of COS was also investigated. The result is shown in Fig. 7. When the flow velocity is 20 mL/min, nearly 100% COS is converted at 150 °C over

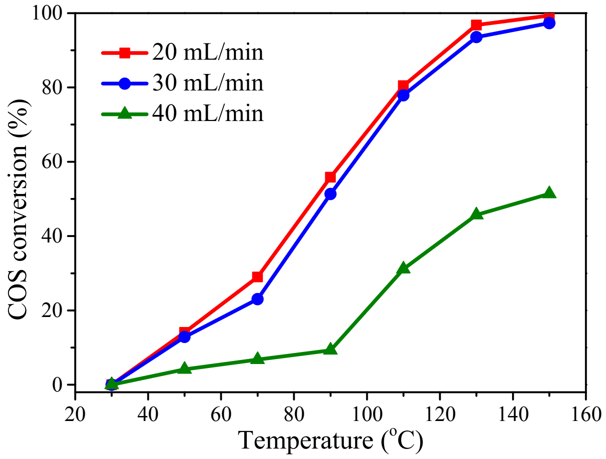

Fig. 7. Influence of flow velocity on COS conversion over HKUST-1-E25. Reaction conditions: catalyst mass 0.4 g, feed gas 100 mg/cm³ COS/N_2, water temperature 40 °C.

HKUST-1-E25. When the flow velocity is increased to 30 mL/min, no significant decrease of the activity is observed: the COS conversion efficiency remains at about 98%. Further increasing the flow velocity leads to a sharp decrease in activity. When the flow velocity is 40 mL/min, only about 50% of COS is converted. The effect of gas flow velocity can be explained as follows. When the flow velocity is too high, insufficient time is available for the catalyst to fully catalyze COS hydrolysis, leading to the decrease of the activity. Therefore, an appropriate flow velocity is necessary for high hydrolysis efficiency of COS.

3.8. The stability of the catalyst

Fig. 8(a) displays the XRD patterns of HKUST-1-E25 before and after the COS hydrolysis reaction. No significant difference in the crystalline structures can be observed, indicating that the structure of HKUST-1-E25 is maintained during the reaction. Fig. 8(b) shows the stability over time of the HKUST-1-E25 and HKUST-1-Hy catalysts. Both samples show considerable stability. After 240 min, about 90% and 70% conversion rates are observed for HKUST-1-E25 and HKUST-1-Hy, respectively. The slight decrease in the activity of HKUST-1 can be attributed to the formation of sulfate on the surface of the catalyst [47]. For the sake of comparison, a Cu/Al_2O_3 (10/90 mass ratio) catalyst was prepared *via* the incipient wetness impregnation method [48], and its activity and stability were tested under the same reaction conditions as HKUST-1. The Cu/A_2O_3 shows high activity for the hydrolysis of COS, as expected. However, as the reaction time is prolonged, Cu/Al_2O_3 shows a marked decrease in activity. After 240 min of reaction, the activity of Cu/Al_2O_3 declines by about 30%. These results demonstrate the advantages of HKUST-1 as a catalyst for COS hydrolysis.

3.9. Reaction mechanism over catalyst

To further analyze the chemical state of the constituent elements and reveal the reaction mechanism, the HKUST-1-E25 samples were characterized by XPS. Fig. 9(a) shows the Cu 2*p* XPS spectra of HKUST-1-E25 before and after reaction. Two characteristic peaks at 934.6 and 954.4 eV are observed, corresponding to the Cu $2p_{3/2}$ and Cu $2p_{1/2}$ states of Cu^{2+}, respectively. Additionally, two "shake-up satellites" located in the 930–965 eV range are generally assigned to Cu^{2+}, another sign that the copper content in HKUST-1 remains in the divalent state, in agreement with a previous report [49]. After the reaction, no obvious change is observed in the Cu 2*p* XPS spectrum, suggesting the good chemical stability of the sample in the reaction process. It should be noted that most copper oxides show poor activity stability in desulfurization reactions, as the strong affinity between copper and sulfur leads to the for-

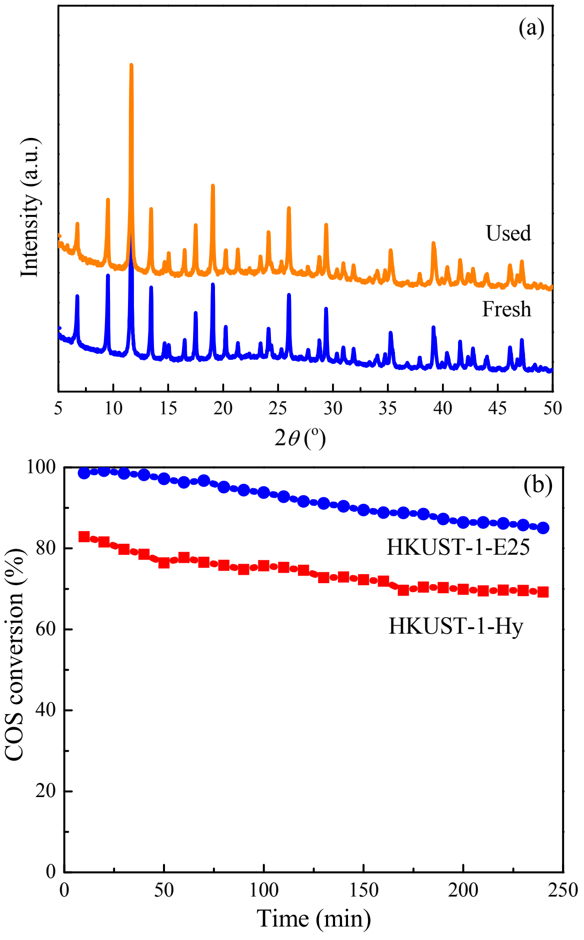

Fig. 8. (a) XRD patterns of fresh and used HKUST-1-E25; (b) COS conversion over HKUST-1-E25 and HKUST-1-Hy.

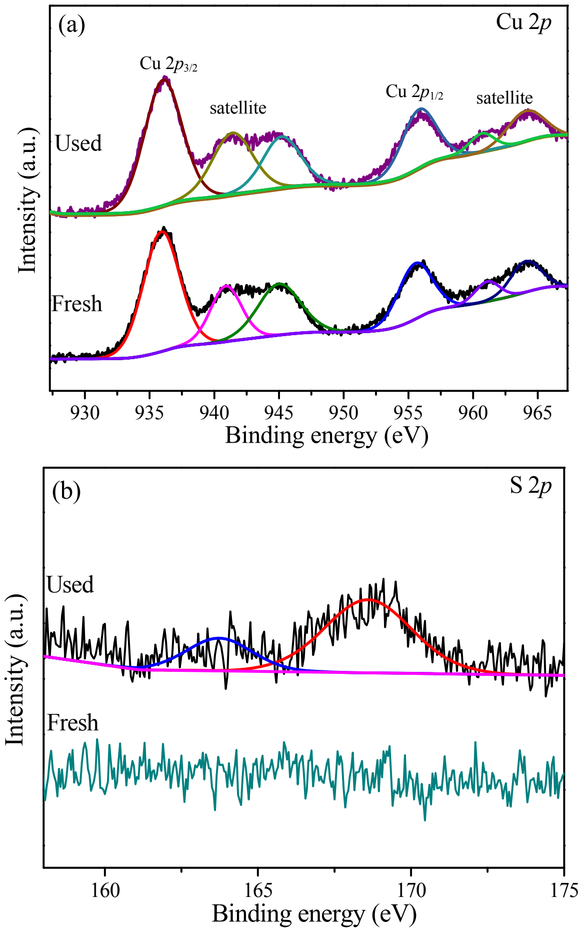

Fig. 9. Cu 2*p* XPS spectra (a) and S 2*p* XPS spectra (b) of HKUST-1-E25 before and after the reaction.

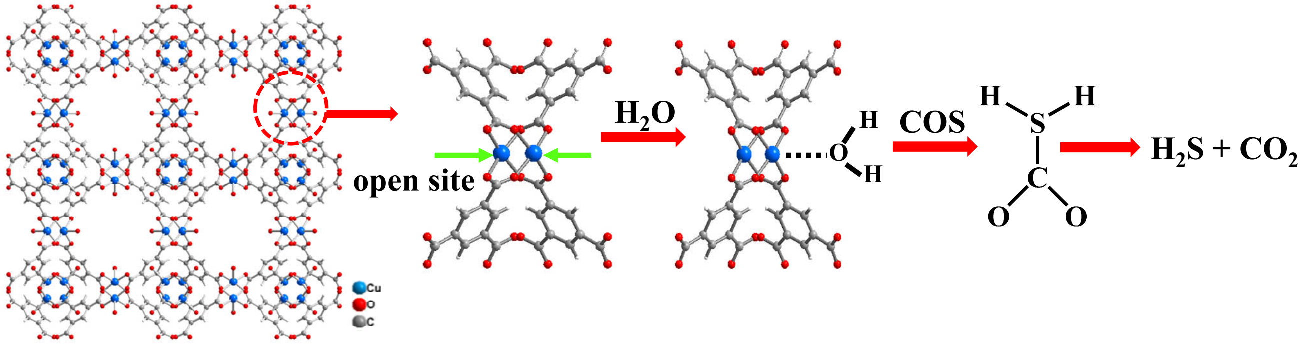

Fig. 10. Possible reaction mechanism of COS hydrolysis over HKUST-1.

mation of CuS. The better stability of HKUST-1 might be attributed to its unique 3D structure. In HKUST-1, dimeric Cu "paddle wheels" are connected to the BTC ligands to form a complicated microporous framework. These stable structures may have inhibited the reaction of Cu^{2+} with S. As a consequence, HKUST-1 shows better sulfate resistance than typical copper oxides. The S 2*p* XPS spectrum of the used sample of HKUST-1-E25 shows two small peaks, at 164 and 169 eV, corresponding to elemental sulfur and sulfate species, respectively [47].

A previous study using density functional theory found that the open-metal sites of HKUST-1 enabled electrostatic interaction between the charge of the open metal and the multipole moments of COS. Meanwhile, H_2O binds with the open-metal sites *via* an acid–base interaction. The adsorption energy of H_2O on the Cu^{2+} sites of HKUST-1 is higher than that of COS [50]. Based on the above discussion and combined with the previous study [11], a possible reaction pathway of COS hydrolysis over HKUST-1 can be tentatively proposed, as shown in Fig. 10. The H_2O molecules are preferentially adsorbed on the open-metal sites of HKUST-1 through the strong acid-base interaction. Then, COS is adsorbed on the remaining open-metal sites through the electrostatic interaction. As the temperature increases, the adsorbed H_2O increasingly reacts with COS, forming H_2S and CO_2. Although the amount of H_2S produced is small, its oxidation to sulfate is considered the main reason for the eventual performance degradation of the catalysts.

4. Conclusions

HKUST-1 has been synthesized by a simple and mild electrochemical method. By controlling the synthesis voltage, the morphology and the catalytic properties of the HKUST-1 can be facilely tuned. The HKUST-1-E25 sample shows the highest efficiency for the hydrolysis of COS, with nearly 100% conversion at 150 °C. This is significantly higher than that of the sample prepared by the hydrothermal method (~60% conversion), demonstrating the benefit of synthesizing MOFs by the electrochemical method. This work is the first example of the use of MOFs for COS hydrolysis. It is hoped that our work could not only offer useful information on the electrochemical fabrication of MOFs but also open a new window on the use of MOFs as catalysts in the growing field of removing sulfur-containing compounds.

References

[1] B. S. Liu, X. N. Wei, Y. P. Zhan, R. Z. Chang, F. Subhan, C. T. Au, *Appl. Catal. B*, **2011**, 102, 27–36.
[2] B. S. Liu, Z. Y. Wan, F. Wang, Y. P. Zhan, M. Tian, A. S. C. Cheung, *J. Hazard. Mater.*, **2014**, 267, 229–237.
[3] G. J. Ma, H. J. Yan, X. Zong, B. J. Ma, H. F. Jiang, F. Y. Wen, C. Li, *Chin. J. Catal.*, **2008**, 29, 313–315.
[4] M. Luo, X. H. Zhang, D. J. Darensbourg, *Acc. Chem. Res.*, **2016**, 49, 2209–2219.
[5] A. Ryzhikov, V. Hulea, D. Tichit, C. Leroi, D. Anglerot, B. Coq, P. Trens, *Appl. Catal. A*, **2011**, 397, 218–224.
[6] Y. X. Ma, X. Q. Wang, P. Ning, C. Cheng, K. Xu, F. Wang, Z. T. Bian, S. D. Yan, *Chem. Eng. J.*, **2016**, 290, 328–334.
[7] H. B. Guo, L. H. Tang, K. Li, P. Ning, J. H. Peng, F. Lu, J. J. Gu, S. Y. Bao, Y. Liu, T. T. Zhu, Z. Y. Duan, *RSC Adv.*, **2015**, 5, 20530–20537.
[8] Z. Q. Yi, X. M. Wang, *J. Environ. Sci.*, **2011**, 23, 784–789.
[9] C. Rhodes, S. A. Riddel, J. West, B. P. Williams, G. J. Hutchings, *Catal. Today*, **2000**, 59, 443–464.
[10] P. D. Clark, N. I. Dowling, M. Huang, *Appl. Catal. B*, **2001**, 31, 107–112.
[11] P. E. Hoggan, A. Aboulayt, A. Pieplu, P. Nortier, J. C. Lavalley, *J. Catal.*, **1994**, 149, 300–306.
[12] H. M. Huang, N. Young, B. P. Williams, S. H. Taylor, G. Hutchings, *Catal. Lett.*, **2006**, 110, 243–246.
[13] B. Thomas, B. P. Williams, N. Young, C. Rhodes, G. J. Hutchings, *Catal. Lett.*, **2003**, 86, 201–205.
[14] J. West, B. P. Williams, N. Young, C. Rhodes, G. J. Hutchings, *Catal. Commun.*, **2001**, 2, 135–138.
[15] H. M. Huang, N. Young, B. P. Williams, S. H. Taylor, G. Hutchings, *Green Chem.*, **2008**, 10, 571–577.
[16] P. Ning, L. L. Yu, H. H. Yi, X. L. Tang, H. Li, H. Y. Wang, L. N. Yang, *J. Rare Earth.*, **2010**, 28, 205–210.
[17] J. Canivet, A. Fateeva, Y. M, Guo, B. Coasne, D. Farrusseng, *Chem. Soc. Rev.*, **2014**, 43, 5594–5617.
[18] A. Schoedel, M. Li, D. Li, M. O'Keeffe, O. M. Yaghi, *Chem. Rev.*, **2016**, 116, 12466–12535.
[19] S. Lee, E. A. Kapustin, O. M. Yaghi, *Science*, **2016**, 353, 808–811.
[20] X. H. Li, W. L. Guo, Z. H. Liu, R. Q. Wang, H. Liu, *Appl. Surf. Sci.*, **2016**, 369, 130–136.
[21] N. L. Rosi, J. Eckert, M. Eddaoudi, D. T. Vodak, J. Kim, M. O'Keeffe, O. M. Yaghi, *Science*, **2003**, 300, 1127–1129.
[22] Z. P. Chen, L. X. Ling, B. J. Wang, H. L. Fan, S. G. Ju, J. Mi, *Appl. Surf.*

Graphical Abstract

Chin. J. Catal., 2017, 38: 1373–1381 doi: 10.1016/S1872-2067(17)62874-2

Tuning the growth of Cu-MOFs for efficient catalytic hydrolysis of carbonyl sulfide

Lijuan Shen, Gaojie Wang, Xiaoxiao Zheng, Yanning Cao, Yufeng Guo, Ke Lin, Lilong Jiang*
Fuzhou University

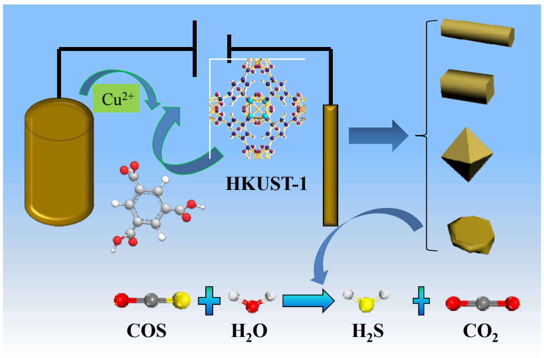

A series of Cu-based metal-organic frameworks (MOFs), HKUST-1, with different morphologies has been controllably synthesized by a mild anodic-dissolution electrochemical method. The obtained samples function as novel and efficient catalysts for COS hydrolysis.

Sci., **2016**, 387, 483–490.
[23] Z. X. Zhao, X. L. Ma, A. Kasik, Z. Li, Y. S. Lin, *Ind. Eng. Chem. Res.*, **2013**, 52, 1102–1108.
[24] S. S. Zhao, J. Yang, Y. Y. Liu, J. F. Ma, *Inorg. Chem.*, **2016**, 55, 2261–2273.
[25] H. Y. Li, Y. L. Wei, X. Y. Dong, S. Q. Zang, T. C. W. Mak, *Chem. Mater.*, **2015**, 27, 1327–1331.
[26] G. Q. Song, Z. Q. Wang, L. Wang, G. R. Li, M. J. Huang, F. X. Yin, *Chin. J. Catal.*, **2014**, 35, 185–195.
[27] P. Pachfule, D. Shinde, M. Majumder, Q. Xu, *Nat. Chem.*, **2016**, 8, 718–724.
[28] J. W. Liu, L. F. Chen, H. Cui, J. Y. Zhang, L. Zhang, C. Y. Su, *Chem. Soc. Rev.*, **2014**, 43, 6011–6061.
[29] M. Zhao, S. Ou, C. D. Wu, *Acc. Chem. Res.*, **2014**, 47, 1199–1207.
[30] L. J. Shen, R. W. Liang, L. Wu, *Chin. J. Catal.*, **2015**, 36, 2071–2088.
[31] L. J. Shen, M. B. Luo, Y. H. Liu, R. W. Liang, F. F. Jing, L. Wu, *Appl. Catal. B*, **2015**, 166–167, 445–453.
[32] M. A. Nasalevich, M. G. Goesten, T. J. Savenije, F. Kapteijn, J. Gascon, *Chem. Commun.*, **2013**, 49, 10575–10577.
[33] L. J. Shen, R. W. Liang, M. B. Luo, F. F. Jing, L. Wu, *Phys. Chem. Chem. Phys.*, **2015**, 17, 117–121.
[34] R. Srirambalaji, S. Hong, R. Natarajan, M. Yoon, R. Hota, Y. Kim, Y. H. Ko, K. Kim, *Chem. Commun.*, **2012**, 48, 11650–11652.
[35] S. Marx, W. Kleist, A. Baiker, *J. Catal.*, **2011**, 281, 76–87.
[36] R. Yepez, S. Garcia, P. Schachat, M. Sanchez-Sanchez, J. H. Gonzalez-Estefan, E. Gonzalez-Zamora, I. A. Ibarra, J. Aguilar-Pliego, *New J. Chem.*, **2015**, 39, 5112–5115.
[37] C. Y. Chuah, K. Goh, T. H. Bae, *J. Phys. Chem. C*, **2017**, 121, 6748–6755.
[38] H. Al-Kutubi, J. Gascon, E. J. R. Sudhölter, L. Rassaei, *ChemElectroChem*, **2015**, 2, 462–474.
[39] M. Hartmann, S. Kunz, D. Himsl, O. Tangermann, S. Ernst, A. Wagener, *Langmuir*, **2008**, 24, 8634–8642.
[40] R. Ameloot, L. Stappers, J. Fransaer, L. Alaerts, B. F. Sels, D. E. De Vos, *Chem. Mater.*, **2009**, 21, 2580–2582.
[41] P. Küsgens, M. Rose, I. Senkovska, H. Fröde, A. Henschel, S. Siegle, S. Kaskel, *Microporous Mesoporous Mater.*, **2009**, 120, 325–330.
[42] A. Martinez Joaristi, J. Juan-Alcañiz, P. Serra-Crespo, F. Kapteijn, J. Gascon, *Cryst. Growth Des.*, **2012**,12, 3489–3498.
[43] Y. T. Wang, Y. Y. Lu, W. W. Zhan, Z. X. Xie, Q. Kuang, L. S. Zheng, *J. Mater. Chem. A*, **2015**, 3, 12796–12803.
[44] C. L. Xin, H. J. Zhan, X. Huang, H. Q. Li, N. Zhao, F. K. Xiao, W. Wei, Y. H. Sun, *RSC Adv.*, **2015**, 5, 27901–27911.
[45] P. D. C. Dietzel, R. E. Johnsen, H. Fjellvag, S. Bordiga, E. Groppo, S. Chavan, R. Blom, *Chem. Commun.*, **2008**, 5125–5127.
[46] Y. Q. Zhang, Z. B. Xiao, J. X. Ma, *Appl. Catal. B*, **2004**, 48, 57–63.
[47] H. Y. Wang, H. H. Yi, X. L. Tang, P. Ning, L. L. Yu, D. He, S. Z. Zhao, K. Li, *Appl. Clay Sci.*, **2012**, 70, 8–13.
[48] A. Bansode, B. Tidona, P. R. von Rohr, A. Urakawa, *Catal. Sci. Technol.*, **2013**, 3, 767–778.
[49] H. Chen, L. F. Wang, J. Yang, R. T. Yang, *J. Phys. Chem. C*, **2013**, 117, 7565–7576.
[50] B. Supronowicz, A. Mavrandonakis, T. Heine, *J. Phys. Chem. C*, **2013**, 117, 14570–14578.

Cu-MOFs的生长调控及其催化水解羰基硫的性能

沈丽娟, 王高杰, 郑笑笑, 曹彦宁, 郭玉峰, 林 科, 江莉龙*
福州大学化肥催化剂国家工程研究中心, 福建福州350002

摘要: 羰基硫(COS)广泛存在于以煤、焦炭、渣油和天然气等为原料生产的化工原料气中, 不仅腐蚀管道设备, 使下游催化剂发生硫中毒, 而且还会造成环境污染. 因此, COS脱除具有重要意义. 在各种方法中, 催化水解COS (COS + $H_2O \rightarrow CO_2 + H_2S$)由于具有反应条件温和、转化率高和副反应少等优点越来越受重视. 其关键在于发展高效的催化剂. 近年来, 金属-有机骨架材料(metal-organic frameworks, MOFs)由于其独特的物理化学性质引起人们广泛关注. 与传统材料相比, MOFs不仅拥有超高的比表面积和规则的孔道结构, 而且其结构具有可设计性强和易调变等特点, 是一类非常有潜力的多相催化剂. 然而, 目前MOFs在催化水解COS方面的研究应用未见报道. 此外, MOFs的合成方法主要有水/溶剂热法、扩散法和微波辅助加热法等. 近年来新发展的电化学法具有合成效率高、操作方便和环境友好等优点, 在材料合成中显示出巨大的优越性, 但利用电化学法合成MOFs相关研究还较少.

本文采用快速温和的电化学方法制备了典型的Cu-MOFs (HKUST-1). 该方法可以有效缩短反应时间, 通过调节反应电压(15–30 V), 在室温下电解3 h, 可得到一系列HKUST-1样品. 根据合成中设置的电压值, 样品分别命名为HKUST-1-E15, HKUST-1-E20, HKUST-1-E25和HKUST-1-E30. XRD表征结果显示, 不同电压下合成样品的XRD谱图与通过晶体数据拟合的HKUST-1图出峰位置基本一致. SEM结果表明, 合成电压对样品形貌的影响很大. HKUST-1-E15主要呈长棒状结构, 长约为15 μm. 随着电压的增大, HKUST-1-E20的形貌逐渐转变为较短的四棱柱体. 当电压为25 V时, 所得HKUST-1-E25呈八面体状. 进一步提高合成电压, HKUST-1-E30颗粒变小, 没有特殊形貌, 并出现明显的团聚. COS水解测试结果显示, 不同电压下合成样品的活性差异大, 这主要是由于样品的形貌及比表面积差异引起的. 其中, HKUST-1-E25样品的活性较好. 在150 °C下, 该样品对COS的转化率接近100%, 比水热法合成的HKUST-1-Hy的活性更高. 在此基础上, 进一步对活性测试过程的条件进行优化, 发现当原料气流速为30 mL/min, 水温为40 °C时, 催化剂的COS水解性能最优. 此外, 样品的活性稳定性测试结果显示, 相比传统的氧化铜材料, HKUST-1是一类较稳定的COS水解催化剂.

关键词: 金属-有机骨架材料; 羰基硫; 电化学合成; 催化水解; HKUST-1

收稿日期: 2017-04-11. 接受日期: 2017-06-17. 出版日期: 2017-08-05.

*通讯联系人. 电话: (0591)83731234; 电子信箱: jll@fzu.edu.cn

基金来源: 国家自然科学基金(21603034, 21576051); 国家高技术研究发展计划(863计划, 2015AA03A402).
本文的英文电子版由Elsevier出版社在ScienceDirect上出版(http://www.sciencedirect.com/science/journal/18722067).